CGI-58 knockdown sequesters diacylglycerols in lipid droplets/ER-preventing diacylglycerol-mediated hepatic insulin resistance

Jennifer L. Cantley[a,b,1], Toru Yoshimura[b,1], Joao Paulo G. Camporez[b], Dongyan Zhang[a,b], Francois R. Jornayvaz[b], Naoki Kumashiro[a,b], Fitsum Guebre-Egziabher[b], Michael J. Jurczak[b], Mario Kahn[a,b], Blas A. Guigni[a,b], Julie Serr[b], Joseph Hankin[c], Robert C. Murphy[c], Gary W. Cline[a,b], Sanjay Bhanot[d], Vara Prasad Manchem[d], J. Mark Brown[e], Varman T. Samuel[b], and Gerald I. Shulman[a,b,f,2]

[a]Howard Hughes Medical Institute and Departments of [b]Internal Medicine and [f]Cellular and Molecular Physiology, Yale School of Medicine, New Haven, CT 06510; [c]Department of Pharmacology, University of Colorado School of Medicine, Denver, CO 80045; [d]Isis Pharmaceuticals, Carlsbad, CA 92010; and [e]Department of Pathology, Wake Forest School of Medicine, Winston-Salem, NC 27157

Contributed by Gerald I. Shulman, November 12, 2012 (sent for review September 25, 2012)

Comparative gene identification 58 (CGI-58) is a lipid droplet-associated protein that promotes the hydrolysis of triglyceride by activating adipose triglyceride lipase. Loss-of-function mutations in CGI-58 in humans lead to Chanarin–Dorfman syndrome, a condition in which triglyceride accumulates in various tissues, including the skin, liver, muscle, and intestines. Therefore, without adequate CGI-58 expression, lipids are stored rather than used for fuel, signaling intermediates, and membrane biosynthesis. CGI-58 knockdown in mice using antisense oligonucleotide (ASO) treatment also leads to severe hepatic steatosis as well as increased hepatocellular diacylglycerol (DAG) content, a well-documented trigger of insulin resistance. Surprisingly, CGI-58 knockdown mice remain insulin-sensitive, seemingly dissociating DAG from the development of insulin resistance. Therefore, we sought to determine the mechanism responsible for this paradox. Hyperinsulinemic-euglycemic clamp studies reveal that the maintenance of insulin sensitivity with CGI-58 ASO treatment could entirely be attributed to protection from lipid-induced hepatic insulin resistance, despite the apparent lipotoxic conditions. Analysis of the cellular compartmentation of DAG revealed that DAG increased in the membrane fraction of high fat-fed mice, leading to PKCε activation and hepatic insulin resistance. However, DAG increased in lipid droplets or lipid-associated endoplasmic reticulum rather than the membrane of CGI-58 ASO-treated mice, and thus prevented PKCε translocation to the plasma membrane and induction of insulin resistance. Taken together, these results explain the disassociation of hepatic steatosis and DAG accumulation from hepatic insulin resistance in CGI-58 ASO-treated mice, and highlight the importance of intracellular compartmentation of DAG in causing lipotoxicity and hepatic insulin resistance.

nonalcoholic fatty liver disease | type 2 diabetes

Nonalcoholic fatty liver disease (NAFLD) is now the most common chronic liver disease in the United States and is strongly associated with hepatic insulin resistance and type 2 diabetes (1, 2). Although NAFLD is characterized by excessively high triglycerides in the liver, the triglycerides do not appear to be detrimental to hepatic insulin sensitivity (3, 4). Rather, other lipid moieties, such as diacylglycerols (DAG) and ceramides, have been implicated as the molecular triggers of insulin resistance (5–7). The mechanism whereby these lipids cause insulin resistance are diverse: DAGs cause insulin resistance through activation of PKCε in liver, leading to the inhibition of insulin-receptor kinase activity (8, 9), and PKCθ in skeletal muscle, leading to insulin-receptor substrate-1 serine phosphorylation on sites that interfere with insulin action (10–12). Ceramides have been proposed to inhibit AKT2 activation by either activating PP2A, which dephosphorylates and deactivates AKT2, or activating PKCζ, which phosphorylates AKT on an inhibitory residue and prevents its translocation to the plasma membrane (5, 13–15).

Although elevated hepatic triglyceride and DAG content are strongly associated with hepatic insulin resistance in humans (16, 17) and most animal models of NAFLD (18), a few mouse models have recently been described where hepatic DAG content has been disassociated from hepatic insulin resistance (19–21), thus challenging the role of hepatic DAGs in mediating hepatic insulin resistance. One of these models is the comparative gene identification-58 (CGI-58) antisense oligonucleotide (ASO) -treated mouse (20). Also known as α/β-hydrolase domain-containing protein 5, CGI-58 is a powerful regulator of triglyceride hydrolysis by coactivating adipose triglyceride lipase (ATGL) (22, 23), which is required for lipolysis (24). ASO-mediated knockdown of hepatic CGI-58 expression therefore leads to a profound increase in both hepatic triglyceride content and DAG content. However, despite increased hepatic DAG content, the ASO-treated mice remain more glucose tolerant and insulin sensitive than control mice when fed a high-fat diet (20). However, the physiologic and cellular mechanisms responsible for this protection from lipid-induced whole body insulin resistance remain unknown.

To address these questions, we performed hyperinsulinemic-euglycemic clamps combined with radiolabeled glucose to examine basal and insulin-stimulated glucose metabolism in liver, muscle, and adipose tissue in control and CGI-58 ASO-treated mice. In addition, because CGI-58 functions at the lipid droplet to regulate lipolysis (23, 25), we also investigated whether knockdown alters the subcellular location of DAG. We found that although CGI-58 ASO treatment led to substantial increases in total DAG content, it is mostly partitioned in the lipid droplet/endoplasmic reticulum (ER), preventing its association with the plasma membrane, activation of PKCε, and induction of hepatic insulin resistance.

Results

CGI-58 ASO Treatment Prevents Diet-Induced Weight Gain and Decreases Adipose Tissue Mass. A critical function of adipocytes is to store excess energy in the form of triglcyeride (26). When energy is required, triglyceride lipolysis releases nonesterified fatty acids for fuel (25–27). Lipases, such as ATGL, are essential

Author contributions: J.L.C., T.Y., J.P.G.C., and G.I.S. designed research; J.L.C., T.Y., J.P.G.C., D.Z., F.R.J., N.K., F.G.-E., M.J.J., M.K., B.A.G., J.S., J.H., R.C.M., and G.W.C. performed research; J.H., R.C.M., S.B., V.P.M., and J.M.B. contributed new reagents/analytic tools; J.L.C., T.Y., J.P.G.C., D.Z., F.R.J., N.K., F.G.-E., M.J.J., M.K., B.A.G., J.S., J.H., R.C.M., G.W.C., V.T.S., and G.I.S. analyzed data; and J.L.C., T.Y., J.P.G.C., D.Z., F.R.J., N.K., F.G.-E., M.J.J., J.H., R.C.M., G.W.C., J.M.B., V.T.S., and G.I.S. wrote the paper.

The authors declare no conflict of interest.

Freely available online through the PNAS open access option.

[1]J.L.C. and T.Y. contributed equally to this work.

[2]To whom correspondence should be addressed. E-mail: gerald.shulman@yale.edu.

This article contains supporting information online at www.pnas.org/lookup/suppl/doi:10.1073/pnas.1219456110/-/DCSupplemental.

for lipolysis and are themselves regulated by a number of proteins, such as CGI-58 (22, 23). Because adipocytes require ATGL for lipolysis (24), it was initially expected that CGI-58 knockdown would result in decreased lipolysis, increased triglyceride storage, and increased weight gain.

As expected, CGI-58 ASO treatment significantly reduced CGI-58 protein expression in the liver and moderately reduced expression in the white adipose tissue (WAT) (Fig. 1 *A* and *B*). The knockdown of CGI-58 caused a tendency toward less weight gain in high fat-fed mice, but did not alter weight gain in regular chow-fed mice (Fig. 1*C*). Although there were no changes in the percent fat mass or lean mass, CGI-58 ASO caused a 40% reduction in epididymal WAT weight in mice fed a high-fat diet (Fig. 1 *D–F*). Additionally, on a regular chow diet, CGI-58 ASO-treated mice also had less epididymal WAT weight, but no change in the percent fat mass or lean mass (Fig. 1 *D–F*). Despite these reductions in WAT, hepatic triglyceride content increased three- to fourfold with CGI-58 ASO treatment on a regular chow and high-fat diet (Fig. 1*G*). Taken together, these data suggest that there may be a repartitioning of lipid away from the epididymal adipose tissue and into the liver with CGI-58 knockdown.

CGI-58 ASO Treatment Protects Mice from Lipid-Induced Hepatic Insulin Resistance, Despite Increased Hepatic Triacylglycerol and DAG Content. Previous studies have shown that ASO-mediated knockdown of CGI-58 prevents high-fat diet-induced obesity and glucose intolerance despite causing severe hepatic steatosis (20). However, because hepatic steatosis most often leads to hepatic insulin resistance and glucose intolerance, we sought to determine the cellular mechanism that might explain the dissociation of hepatic steatosis from insulin resistance with CGI-58 knockdown. To determine which insulin-responsive tissues are responsible for the protective effect of CGI-58 knockdown, we performed hyperinsulinemic-euglycemic clamp studies using radio-labeled glucose to examine insulin action in liver, muscle, and adipose tissue.

There were no significant differences in fasting-plasma glucose levels or basal rates of endogenous glucose production in control or CGI-58 ASO-treated mice fed either a regular chow diet or a high-fat diet following 6 h of food removal (Fig. 2 *A* and *F*). Although there was a reduction in fasting-plasma insulin concentrations with CGI-58 ASO treatment on a regular chow diet, there were no differences in the fasting-plasma insulin levels on a high-fat diet (Fig. 2*B*).

Surprisingly, despite the striking increase in hepatic triglyceride content (Fig. 1*G*), CGI-58 ASO-treated mice maintained normal insulin responsiveness when fed a regular chow diet, as reflected by no differences between the glucose infusion rate required to maintain euglycemia between the groups (Fig. 2 *C* and *D*). In high fat-fed mice, CGI-58 ASO treatment increased insulin responsiveness compared with the control ASO, as reflected by a 45% higher glucose infusion rate required to maintain euglycemia during the hyperinsulinemic-euglycemic clamp (Fig. 2 *C* and *D*). This protection from lipid-induced whole-body insulin resistance could entirely be attributed to protection from lipid-induced hepatic insulin resistance. Notably, there was almost complete suppression of endogenous glucose production during the hyperinsulinemic-euglycemic clamp in both the regular chow and high fat-fed CGI-58 ASO-treated mice compared with only 50% suppression of endogenous glucose production in the high fat-fed control mice (Fig. 2 *F* and *G*). Additionally, both high fat-fed control and CGI-58 ASO-treated mice had a 25–35% reduction in insulin-stimulated peripheral glucose metabolism, indicating that peripheral tissues were not contributing to the increased insulin-stimulated whole-body glucose metabolism observed in CGI-58 knockdown mice (Fig. 2*E*). Furthermore, consistent with the clamp data, CGI-58 knockdown mice maintained insulin-stimulated AKT2 phosphorylation, but high fat-fed control mice had a 40% reduction in insulin-stimulated AKT2 phosphorylation (Fig. 3). Taken together, these data show that the CGI-58 ASO-treated mice are protected from lipid-induced insulin resistance by maintaining insulin signaling and sensitivity in the liver, but not by increasing insulin-stimulated peripheral glucose disposal. These latter results are in accordance with the studies of Lord et al., who found that CGI-58 knockdown had no effect on muscle or white adipose tissue insulin-stimulated AKT phosphorylation (28).

CGI-58 Knockdown Enhances Adipocyte Function with High-Fat Diet. Although insulin-stimulated whole-body glucose disposal was not affected with CGI-58 ASO treatment, adipocyte function did appear to be enhanced in the CGI-58 ASO-treated mice, as reflected by a twofold increase in insulin-stimulated suppression of plasma fatty acids in CGI-58 ASO-treated mice compared with high fat-fed control mice (Fig. 4 *A* and *B*). Additionally, plasma concentrations of adiponectin were increased by ~50% in the CGI-58 ASO-treated mice on regular chow or high-fat diet (Fig. 4*C*). Because this adipocyte-secreted protein typically decreases in serum when adipocyte function is compromised (26, 29, 30), these data suggest that adipocyte function is enhanced with CGI-58 knockdown.

CGI-58 Knockdown Leads to Increased DAG Accumulation in the Lipid Droplet/ER, Preventing DAG Accumulation and PKCε Translocation to the Plasma Membrane. Although CGI-58 ASO led to a marked increase in hepatic triglyceride content (Fig. 1*G*), triglyceride has

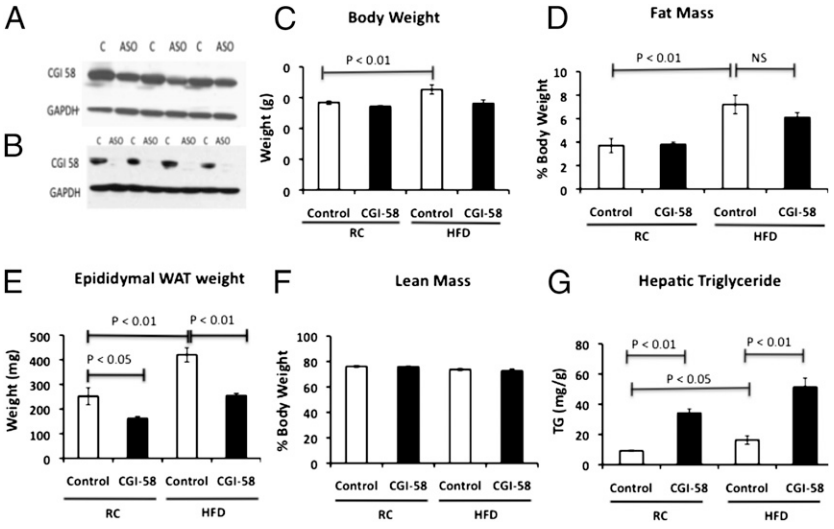

Fig. 1. CGI-58 ASO treatment decreases adiposity and diet induced weight gain, but causes severe hepatic steatosis. Eight-week-old mice were treated with control or CGI-58 ASO for 8 wk and (*A*) CGI-58 protein expression was analyzed in the WAT by Western blot. (*B*) CGI-58 protein expression was analyzed in the liver. (*C*) Body weight. (*D*) Fat mass of the epididymal WAT as assessed by ^{1}H magnetic resonance spectroscopy. (*E*) Epididymal WAT weight. (*F*) Lean mass assessed by ^{1}H magnetic resonance spectroscopy. (*G*) Hepatic triglyceride content. *P* value was calculated by two-way ANOVA.

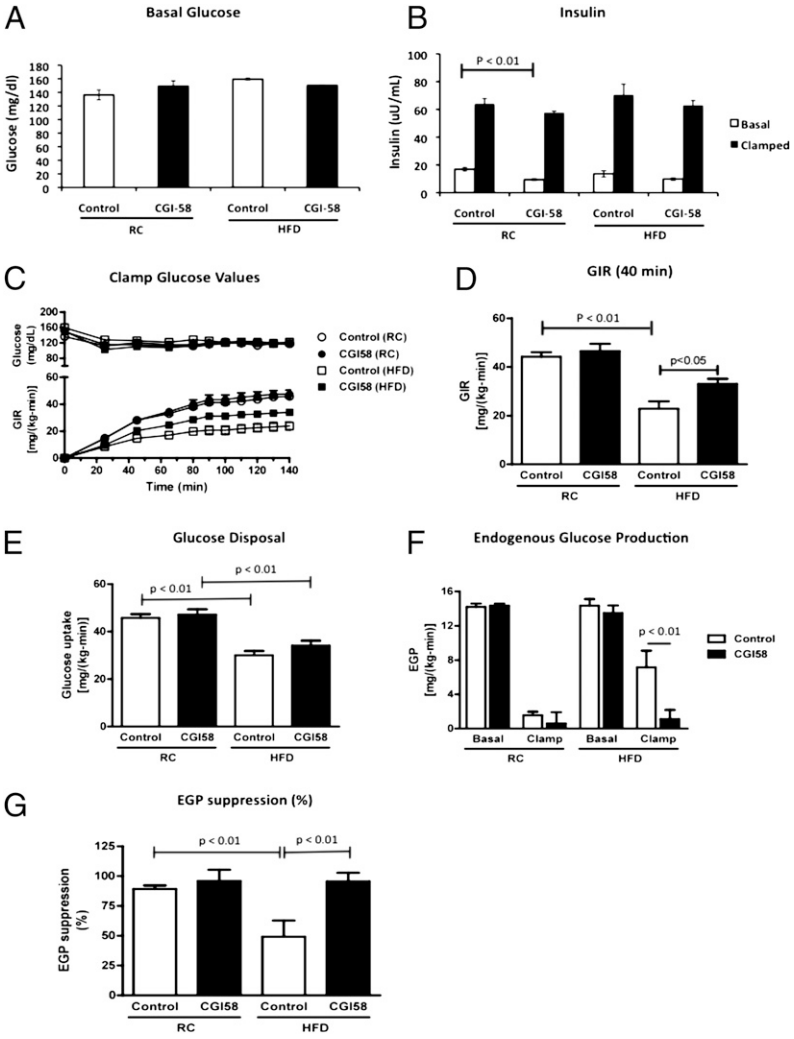

Fig. 2. Loss of CGI-58 expression prevents diet-induced insulin resistance by increasing hepatic insulin sensitivity. (*A*) Basal glucose levels in overnight-fasted mice treated with control or CGI-58 ASO for 8 wk. (*B*) Insulin levels before and after the hyperinsulinemic-euglycemic clamp studies in mice treated with control or CGI-58 ASO for 8 wk. (*C*) Glucose infusion rates required to maintain euglycemia during the hyperinsulinemic-euglycemic clamp studies. (*D*) Average of the glucose infusion rates required to maintain euglycemia during the hyperinsulinemic-euglycemic clamp studies during the last 40 min of the clamp. (*E*) Insulin-stimulated peripheral glucose disposal during the hyperinsulinemic-euglycemic clamp studies. (*F*) Endogenous glucose production during the hyperinsulinemic-euglycemic clamp studies. (*G*) Insulin-stimulated suppression of endogenous glucose production during the hyperinsulinemic-euglycemic clamp studies (n = 8–10 per group). P value calculated by two-way ANOVA.

been shown to be dissociated from insulin resistance (12). Thus, we measured the concentration of DAG, because this intracellular lipid metabolite has been well-documented to cause insulin resistance in both liver and skeletal muscle through activation of PKCε and PKCθ, respectively (8, 9). We found that CGI-58 knockdown led to an approximate twofold increase in

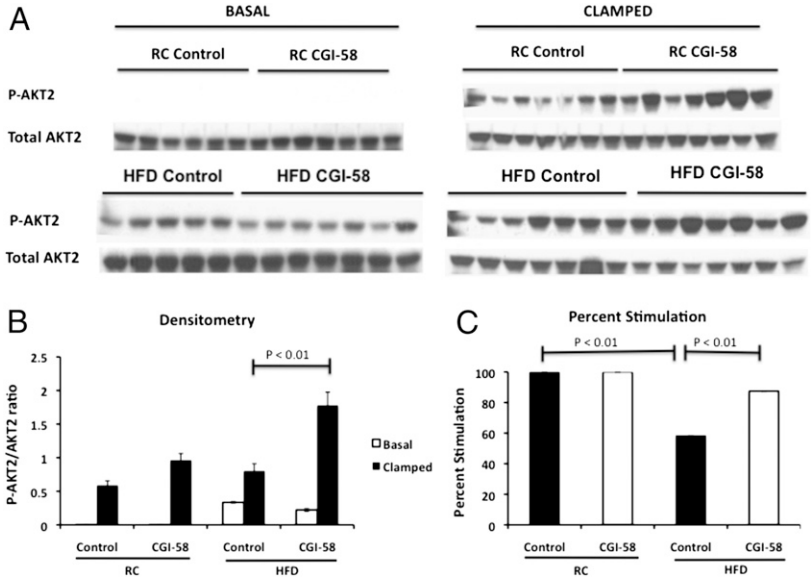

Fig. 3. Hepatic insulin signaling is enhanced with CGI-58 knockdown. (*A*) Western blot analysis of phosphorylated AKT2 (Ser474) in the liver of control or CGI-58 ASO-treated mice in the basal or clamped state. Twenty micrograms of protein were run on a SDS/PAGE gel. (*B*) Densitometry of the phosphorylated AKT2 described in *A*. (*C*) The percent stimulation of AKT2 phosphorylation between the basal and insulin-stimulated states as determined by densitometry. P value was calculated by two-way ANOVA.

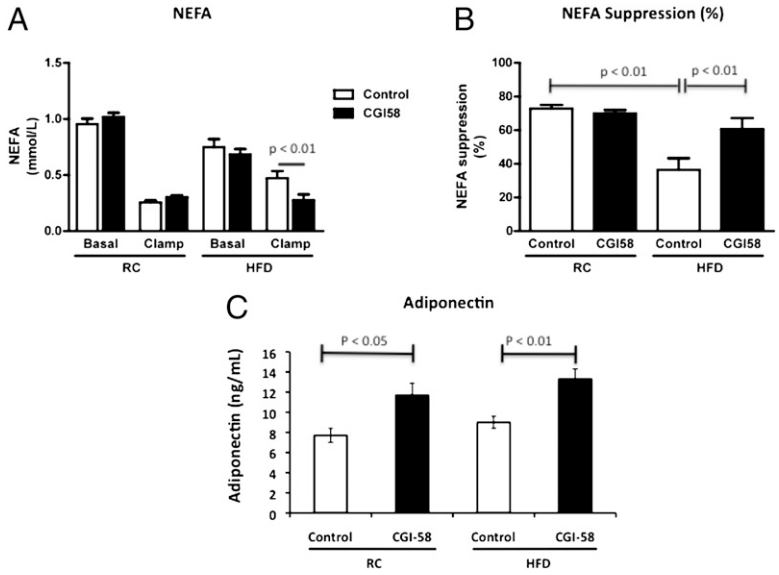

Fig. 4. Adipocyte function is enhanced with CGI-58 knockdown. (*A*) Serum levels of nonesterified fatty acids before and after the hyperinsulinemic-euglycemic clamp studies in mice treated with control or CGI-58 ASO for 8 wk. (*B*) Insulin-stimulated suppression of nonesterifed fatty acid release into the serum during the hyperinsulinemic-euglycemic clamp studies (n = 8–10 per group). (*C*) Serum levels of adiponectin from mice in the basal state treated with control or CGI-58 ASO for 8 wk (n = 5–8 per group). *P* value calculated by two-way ANOVA.

hepatic DAG content, consistent with previous observations (20) (Fig. 5*A*).

Given that ATGL functions at the surface of lipid droplets and has a low level of activity in the absence of CGI-58 (23, 25), we hypothesized that CGI-58 knockdown leads to DAG accumulation in lipid droplets, possibly because of the incomplete lipolysis of triglyceride. Under this scenario, DAG would mostly accumulate in lipid droplets rather than in the plasma membrane, preventing PKCε translocation to the plasma membrane, and induction of hepatic insulin resistance. To determine the intracellular location of DAG, fresh liver tissue homogenate was separated into three fractions (membrane, cytoplasm, and lipid droplet/ER) by ultracentrifugation and DAG content was quantified in each fraction. In insulin-resistant, high fat-fed mice, a 50% increase in hepatic DAG was found specifically in the membrane fraction. In contrast, the CGI-58 ASO-treated mice had a fourfold and eightfold increase in DAG content in the lipid droplet/ER fraction with regular chow and high-fat diet, respectively, but no change in DAG content in the cytoplasm or membrane fractions (Fig. 5 *B–D*).

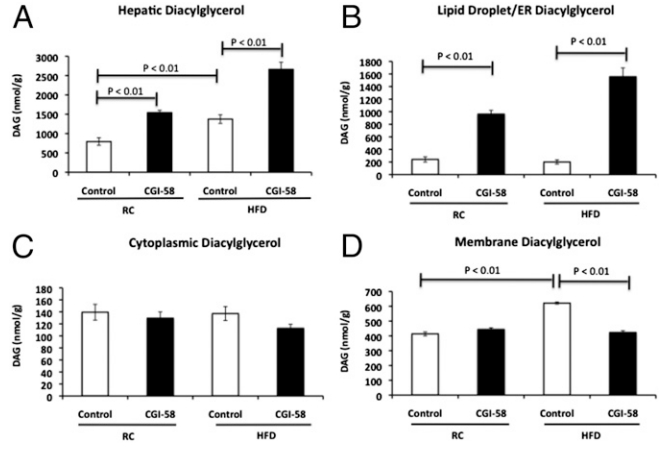

Fig. 5. CGI-58 ASO treatment causes diacylglyerol accumulation in the lipid droplet/ER, but not in the membrane. (*A*) Hepatic DAG concentrations as assessed by LC/MS/MS in mice treated with control or CGI-58 ASO for 8 wk (n = 8 per group). (*B*) DAG concentration in the lipid droplet/ER fraction. (*C*) DAG concentration in the cytoplasmic fraction. (*D*) DAG concentration in the membrane fraction (n = 6 per group). *P* value calculated by two-way ANOVA.

To determine if this repartitioning of DAG with CGI-58 knockdown causes PKCε translocation to the lipid droplet/ER fraction rather than the membrane, we analyzed PKCε levels in these two fractions. As seen in Fig. 6, PKCε strikingly increased in the lipid droplet/ER fraction with CGI-58 knockdown, but did not increase in the high fat-fed control mice. Conversely, PKCε association with the membrane increased by 30% in high fat-fed control mice compared with regular chow-fed control mice, while PKCε association with the membrane in CGI-58 ASO-treated mice was similar to regular chow-fed control mice, even when fed a high-fat diet. Therefore, these data are consistent with the hypothesis that repartitioning of DAG from the membrane to the lipid droplet/lipid-associated ER fraction prevented PKCε translocation to the membrane, thereby averting the induction of hepatic insulin resistance in CGI-58 ASO-treated mice.

CGI-58 ASO Treatment Increases Hepatic Ceramide Content in the Lipid Droplet/ER and Membrane. Ceramides have also been implicated as a causal factor in the development of hepatic insulin resistance by inhibiting AKT activity (5, 13–15) and were increased in CGI-58 ASO-treated mice (20). Therefore, we analyzed hepatic ceramide species and content to determine whether ceramide repartitions to the lipid droplet/ER similar to DAG in the CGI-58 knockdown mice. Although there was no change in total hepatic ceramide content in the high fat-fed control mice, there was a 45% and 67% increase in hepatic ceramide content in CGI-58 ASO-treated mice fed a regular chow and high-fat diet, respectively (Fig. 7*A*). However, in contrast to the DAG findings, the hepatic ceramide content in the CGI-58 ASO-treated mice was increased in all cellular fractions (lipid droplet/ER, cytoplasm, and membrane fractions). These results demonstrate that, in contrast to DAG, CGI-58 knockdown results in a global increase in hepatic ceramide content, without the cellular repartitioning of ceramide into these different cellular compartments. Furthermore, the increase in hepatic ceramide content in both the regular chow and high fat-fed CGI-58 ASO-treated mice was disassociated from the induction of hepatic insulin resistance in these animals.

Discussion

Lipid droplets are dynamic organelles that consist of an inert lipid core surrounded by a phospholipid monolayer (31, 32). Many proteins associate with lipid droplets and control the storage or release of lipid used for energy, membrane biosynthesis, and signaling. Therefore, by controlling intracellular

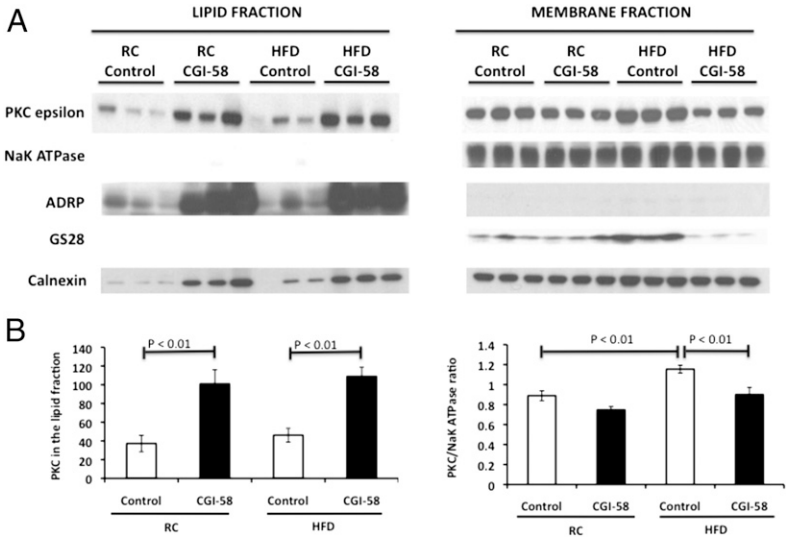

Fig. 6. PKCε translocates to the lipid droplet/ER rather than the membrane with CGI-58 knockdown. (*A*) Western blot analysis of PKCε in the lipid droplet/ER fraction and membrane fraction in mice treated with control or CGI-58 ASO for 8 wk. NaK ATPase (plasma membrane), ADRP (lipid droplet), GS28 (golgi apparatus), and calnexin (ER) ($n = 6$ per group). (*B*) Densitometry of the PKCε described in *A*. *P* value calculated by two-way ANOVA.

lipid levels, lipid droplets greatly impact lipid metabolism, glucose metabolism, and insulin signaling (25, 27, 31, 32).

One protein that associates with lipid droplets and controls triglyceride hydrolysis is CGI-58. This protein is a coactivator of the triglyceride lipase, ATGL, and facilitates lipolysis (22, 23, 25). Because depletion of ATGL results in an obese mouse, it was initially assumed that depletion of CGI-58 would cause a similar phenotype (24, 33). In contrast, previous studies have shown that CGI-58 ASO treatment results in less weight gain and lower epididymal adipose tissue weight (20). This decrease in WAT weight may be a result of decreased lipid delivery to the WAT and therefore triacylglycerol (TAG) storage, because both plasma triglyceride level and hepatic triglyceride secretion rate are decreased with CGI-58 ASO treatment (20).

Because whole-body knockout of the gene encoding CGI-58 leads to a neonatal lethal skin-barrier defect (34), we treated adult mice with CGI-58 ASO to knock down CGI-58 expression mostly in the liver and adipose tissue. We found that CGI-58 ASO treatment protected mice from lipid-induced hepatic insulin resistance despite profound increases in hepatic TAG, DAG, and ceramide content. Although intracellular TAG content has clearly been disassociated from insulin resistance in previous studies (12), both intracellular DAG and ceramide content have been implicated as the molecular mediators of lipid-induced insulin resistance (2, 7, 9, 13, 14). Therefore, the current studies were undertaken to explain the paradoxical lack of hepatic insulin resistance in the presence of increased hepatic DAG and ceramide content with CGI-58 ASO treatment.

Because CGI-58 regulates lipid droplet lipolysis (23), we hypothesized that the elevated DAG content found with CGI-58 knockdown may be stored and compartmentalized in lipid droplets, rather than accumulating in the plasma membrane. Redirecting DAGs in this manner would prevent activation of PKCε at the plasma membrane, where it inhibits insulin-receptor kinase activity and downstream insulin signaling (2, 4, 6–9). Therefore, we performed cell-fractionation studies to determine DAG localization in the membrane, cytoplasm, and lipid droplet/ER fractions, and found that DAG was indeed enriched in the lipid droplet/ER fraction with CGI-58 knockdown. In fact, maintaining DAG in the lipid droplet/ER compartment prevented DAG membrane accumulation and PKCε membrane translocation with CGI-58 knockdown.

Because lipid droplets originate in the ER (31), and CGI-58 ASO treatment stresses the lipid droplet biosynthesis pathway, we could not fully separate lipid droplets from the ER fraction. Therefore, it is always possible that DAG is accumulating in some portion of the ER and not actually in lipid droplets with CGI-58 knockdown. However, these data demonstrate that PKCε is sequestered in this lipid-rich compartment and prevented from translocating to the plasma membrane to inhibit insulin-receptor kinase activity and induce hepatic insulin resistance.

Although the repartitioning of DAG away from the membrane and into the lipid droplet/ER fraction explains the apparent disassociation of increased hepatic DAG content and the lack of hepatic insulin resistance in the CGI-58 ASO-treated mice, this was not the case with hepatic ceramide. In fact, hepatic ceramide content was elevated in all cellular compartments in regular chow-fed and high fat-fed CGI-58 ASO-treated mice despite the lack of hepatic insulin resistance. Additionally, although control mice developed hepatic insulin resistance after 7 d on the high-fat diet, they did not have increased total hepatic ceramide levels. Taken together, these data do not support a major role for hepatic ceramides in causing hepatic insulin resistance and are consistent with previous studies in both rodents and humans (2, 6, 7, 16).

We explored potential mechanisms that could account for the increase in DAG content with CGI-58 knockdown by measuring

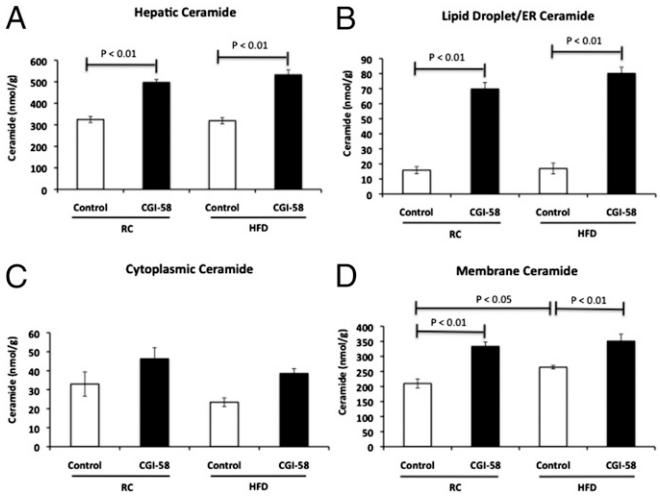

Fig. 7. CGI-58 ASO treatment increases hepatic ceramide content in the lipid droplet/ER and membrane. (*A*) Hepatic ceramide concentrations as assessed by LC/MS/MS in mice treated with control or CGI-58 ASO for 8 wk ($n = 8$ per group). (*B*) Ceramide concentration in the lipid droplet/ER fraction. (*C*) Ceramide concentration in the cytoplasmic fraction. (*D*) Ceramide concentration in the membrane fraction ($n = 6$ per group). *P* value calculated by two-way ANOVA.

the expression of genes that regulate DAG production. Gene-expression analysis shows that AGPAT and glycerol-3-phosphate acyltransferase 3, but not DGAT, increased nearly threefold in expression (Fig. S1). This process could accelerate monoglyceride and DAG synthesis, but not triglyceride synthesis, causing a build up of DAG. Conversely, incomplete lipolysis of triglyceride may also be contributing to DAG generation, because ATGL expression increases with CGI-58 knockdown (Fig. S1) and can function at a low level without CGI-58 (23). However, recent evidence suggests that ATGL generates sn-1,3 DAG and when in the presence of CGI-58 generates sn-2,3 DAG, but does not generate sn-1,2 DAG (35), which is generated through lipid synthesis. Because greater than 95% of DAG is sn-1,2 DAG/sn-2,3 DAG with CGI-58 knockdown (Fig. S2), and sn-2,3 DAG should not be contributing because there is a near ablation of CGI-58 in the liver, it appears that lipid synthesis rather than incomplete lipolysis may be causing DAG accumulation in the lipid droplet/ER fraction with CGI-58 ASO treatment. However, further studies will be required to address this question.

Bergman et al. recently reported that certain DAG species, such as 16:0/18:1 and 16:1/18:1, best correlate with PKCε activation in human muscle (17), indicating that PKCε may respond to these DAG species more than others. However, we found there was a general increase in all DAG species in the lipid droplet/ER with knockdown and most DAG species in the membrane of high fat diet control mice (Fig. S3). Therefore, we did not find a specific membrane DAG species that would fit this model. Alternatively, it is possible that the position of the fatty-acid species on the glycerol backbone of DAG could cause differences in PKCε activation. However, as noted above we found that greater than 95% of the DAG is likely to be sn-1,2 DAG rather than sn-1,3 DAG in control and CGI-58 ASO-treated mice. Therefore, neither differences in DAG species nor stereochemistry of DAG appear to explain the protection from lipid-induced hepatic insulin resistance seen with CGI-58 knockdown.

We recently reported that DAG content in the cytoplasmic/lipid droplet fraction best correlated with insulin resistance in obese humans (16). Here we show that membrane DAG is the best predictor of insulin resistance in high fat-fed mice, and lipid droplets appear to act as a neutral storage depot for DAGs. There are potentially several explanations for this difference. Humans typically develop NAFLD and hepatic insulin resistance over a longer period than the 7 d of high-fat feeding used to induce NAFLD in mice in the present study, which may alter the localization of DAG accumulation. Alternatively, differences in tissue processing (e.g., procurement, fractionation) may have altered DAG localization, masking a potential relationship between membrane DAG and insulin resistance in the human samples. Finally, the discrepancy could simply be because of species differences.

In summary, we found that CGI-58 ASO treatment promotes sequestering of hepatic DAG in the lipid droplet/ER fraction and a repartitioning of DAG away from plasma membrane, abrogating PKCε translocation to the plasma membrane and hepatic insulin resistance. Taken together, these results explain the paradoxical disassociation of hepatic steatosis and hepatic DAG accumulation from hepatic insulin resistance in CGI-58 ASO-treated mice, and highlight the importance of intracellular compartmentation of DAG in causing hepatic insulin resistance in this model and potentially other models of hepatic steatosis.

Methods

See *SI Methods* for a detailed description of the methods used. The methods describe animal and ASO treatment, hyperinsulinemic-euglycemic clamp studies, biochemical analysis and calculations, tissue lipid measurement, RNA preparation and RT-PCR analysis, immunoblotting, cell fractionation, and statistical analysis.

ACKNOWLEDGMENTS. We thank Aida Groszmann for excellent technical assistance and Dr. Fred Gorelick for helpful discussions. This work was support by National Institutes of Health Grants R24 DK-059635, R01 DK-40936, P30 DK-45735, and U24 DK-059635; a VA Merit Award (5101BX000901); the Uehara Memorial Foundation and the Arata Clinic, Nagasaki, Japan; and a Mentor-Based Postdoctoral Fellowship Award from the American Diabetes Association.

1. Cheung O, Sanyal AJ (2010) Recent advances in nonalcoholic fatty liver disease. *Curr Opin Gastroenterol* 26(3):202–208.
2. Samuel VT, Shulman GI (2012) Mechanisms for insulin resistance: Common threads and missing links. *Cell* 148(5):852–871.
3. Neschen S, et al. (2007) n-3 Fatty acids preserve insulin sensitivity in vivo in a peroxisome proliferator-activated receptor-alpha-dependent manner. *Diabetes* 56(4):1034–1041.
4. Shulman GI (2000) Cellular mechanisms of insulin resistance. *J Clin Invest* 106(2):171–176.
5. Bikman BT, Summers SA (2011) Ceramides as modulators of cellular and whole-body metabolism. *J Clin Invest* 121(11):4222–4230.
6. Jornayvaz FR, Shulman GI (2012) Diacylglycerol activation of protein kinase Cε and hepatic insulin resistance. *Cell Metab* 15(5):574–584.
7. Samuel VT, Petersen KF, Shulman GI (2010) Lipid-induced insulin resistance: Unravelling the mechanism. *Lancet* 375(9733):2267–2277.
8. Samuel VT, et al. (2004) Mechanism of hepatic insulin resistance in non-alcoholic fatty liver disease. *J Biol Chem* 279(31):32345–32353.
9. Samuel VT, et al. (2007) Inhibition of protein kinase Cepsilon prevents hepatic insulin resistance in nonalcoholic fatty liver disease. *J Clin Invest* 117(3):739–745.
10. Griffin ME, et al. (1999) Free fatty acid-induced insulin resistance is associated with activation of protein kinase C theta and alterations in the insulin signaling cascade. *Diabetes* 48(6):1270–1274.
11. Li Y, et al. (2004) Protein kinase C Theta inhibits insulin signaling by phosphorylating IRS1 at Ser(1101). *J Biol Chem* 279(44):45304–45307.
12. Yu C, et al. (2002) Mechanism by which fatty acids inhibit insulin activation of insulin receptor substrate-1 (IRS-1)-associated phosphatidylinositol 3-kinase activity in muscle. *J Biol Chem* 277(52):50230–50236.
13. Chavez JA, Summers SA (2012) A ceramide-centric view of insulin resistance. *Cell Metab* 15(5):585–594.
14. Holland WL, et al. (2007) Inhibition of ceramide synthesis ameliorates glucocorticoid-, saturated-fat-, and obesity-induced insulin resistance. *Cell Metab* 5(3):167–179.
15. Schmitz-Peiffer C (2010) Targeting ceramide synthesis to reverse insulin resistance. *Diabetes* 59(10):2351–2353.
16. Kumashiro N, et al. (2011) Cellular mechanism of insulin resistance in nonalcoholic fatty liver disease. *Proc Natl Acad Sci USA* 108(39):16381–16385.
17. Bergman BC, Hunerdosse DM, Kerege A, Playdon MC, Perreault L (2012) Localisation and composition of skeletal muscle diacylglycerol predicts insulin resistance in humans. *Diabetologia* 55(4):1140–1150.
18. Anstee QM, Goldin RD (2006) Mouse models in non-alcoholic fatty liver disease and steatohepatitis research. *Int J Exp Pathol* 87(1):1–16.
19. Benhamed F, et al. (2012) The lipogenic transcription factor ChREBP dissociates hepatic steatosis from insulin resistance in mice and humans. *J Clin Invest* 122(6):2176–2194.
20. Brown JM, et al. (2010) CGI-58 knockdown in mice causes hepatic steatosis but prevents diet-induced obesity and glucose intolerance. *J Lipid Res* 51(11):3306–3315.
21. Sun Z, et al. (2012) Hepatic Hdac3 promotes gluconeogenesis by repressing lipid synthesis and sequestration. *Nat Med* 18(6):934–942.
22. Lass A, et al. (2006) Adipose triglyceride lipase-mediated lipolysis of cellular fat stores is activated by CGI-58 and defective in Chanarin-Dorfman Syndrome. *Cell Metab* 3(5):309–319.
23. Lu X, Yang X, Liu J (2010) Differential control of ATGL-mediated lipid droplet degradation by CGI-58 and G0S2. *Cell Cycle* 9(14):2719–2725.
24. Haemmerle G, et al. (2006) Defective lipolysis and altered energy metabolism in mice lacking adipose triglyceride lipase. *Science* 312(5774):734–737.
25. Wang S, et al. (2008) Lipolysis and the integrated physiology of lipid energy metabolism. *Mol Genet Metab* 95(3):117–126.
26. Guilherme A, Virbasius JV, Puri V, Czech MP (2008) Adipocyte dysfunctions linking obesity to insulin resistance and type 2 diabetes. *Nat Rev Mol Cell Biol* 9(5):367–377.
27. Christianson JL, Boutet E, Puri V, Chawla A, Czech MP (2010) Identification of the lipid droplet targeting domain of the Cidea protein. *J Lipid Res* 51(12):3455–3462.
28. Lord CC, et al. (2012) CGI-58/ABHD5-derived signaling lipids regulate systemic inflammation and insulin action. *Diabetes* 61(2):355–363.
29. Rabe K, Lehrke M, Parhofer KG, Broedl UC (2008) Adipokines and insulin resistance. *Mol Med* 14(11-12):741–751.
30. Rasouli N, Kern PA (2008) Adipocytokines and the metabolic complications of obesity. *J Clin Endocrinol Metab* 93(11):Suppl 1):S64–S73.
31. Martin S, Parton RG (2006) Lipid droplets: A unified view of a dynamic organelle. *Nat Rev Mol Cell Biol* 7(5):373–378.
32. Wolins NE, Brasaemle DL, Bickel PE (2006) A proposed model of fat packaging by exchangeable lipid droplet proteins. *FEBS Lett* 580(23):5484–5491.
33. Kienesberger PC, et al. (2009) Adipose triglyceride lipase deficiency causes tissue-specific changes in insulin signaling. *J Biol Chem* 284(44):30218–30229.
34. Radner FP, et al. (2010) Growth retardation, impaired triacylglycerol catabolism, hepatic steatosis, and lethal skin barrier defect in mice lacking comparative gene identification-58 (CGI-58). *J Biol Chem* 285(10):7300–7311.
35. Eichmann TO, et al. (2012) Studies on the substrate and stereo/regioselectivity of adipose triglyceride lipase, hormone-sensitive lipase, and diacylglycerol-O-acyltransferases. *J Biol Chem* 287(49):41446–41457.